Article

Discovery of potent and orally bioavailable macrocyclic peptide-peptoid hybrid CXCR7 modulators.

Markus Boehm, Kevin Beaumont, Rhys M Jones, Amit S. Kalgutkar, Liying Zhang, Karen Atkinson, Guoyun Bai, Janice A. Brown, Heather Eng, Gilles H. Goetz, Brian R Holder, Bhagyashree Khunte, Sarah Lazzaro, Chris Limberakis, Sangwoo Ryu, Michael J Shapiro, Laurie Tylaska, Jiangli Yan, Rushia Turner, Siegfried S. F. Leung, Mahesh Ramaseshan, David A. Price, Spiros Liras, Matthew P Jacobson, David J. Earp, R. Scott Lokey, Alan M Mathiowetz, and Elnaz Menhaji-Klotz

J. Med. Chem., **Just Accepted Manuscript** • DOI: 10.1021/acs.jmedchem.7b01028 • Publication Date (Web): 18 Oct 2017

Discovery of potent and orally bioavailable macrocyclic peptide-peptoid hybrid CXCR7 modulators

Markus Boehm,[†] Kevin Beaumont,[†] Rhys Jones,[†] Amit S. Kalgutkar,[†] Liying Zhang,[⊥] Karen Atkinson,[‡] Guoyun Bai,[‡] Janice A. Brown,[‡] Heather Eng,[‡] Gilles H. Goetz,[‡] Brian R. Holder,[‡] Bhagyashree Khunte,[‡] Sarah Lazzaro,[‡] Chris Limberakis,[‡] Sangwoo Ryu,[‡] Michael J. Shapiro,[‡] Laurie Tylaska,[‡] Jiangli Yan,[‡] Rushia Turner,[#] Siegfried S. F. Leung,[§,∥] Mahesh Ramaseshan,[∥] David A. Price,[†] Spiros Liras,[†] Matthew P. Jacobson,[§] David J. Earp,[∥] R. Scott Lokey,*[#] Alan M. Mathiowetz,[†] and Elnaz Menhaji-Klotz*[†]*

Pfizer Worldwide Research & Development, [†]Cambridge, Massachusetts 02139, United States and [‡]Groton, Connecticut 06340, United States

[#]Chemistry and Biochemistry, University of California, Santa Cruz, California 95064, United States

[§]Department of Pharmaceutical Chemistry, University of California, San Francisco, California 94158, United States

[∥]Circle Pharma, South San Francisco, California 94080, United States

KEYWORDS: CXCR7 modulator, peptidic macrocycle, cyclic peptide, peptoid, peptide-peptoid hybrid, arginine replacement, tryptophan substitution, N-methylation, passive permeability, polarity, lipophilicity, oral bioavailability.

ABSTRACT: The chemokine receptor CXCR7 is an attractive target for a variety of diseases. While several small molecule modulators of CXCR7 have been reported, peptidic macrocycles may provide advantages in terms of potency, selectivity, and reduced off-target activity. We produced a series of peptidic macrocycles that incorporate an N-linked peptoid functionality where the peptoid group enabled us to explore side chain diversity well beyond that of natural amino acids. At the same time, computational calculations and experimental assays were used to track and reduce polarity while closely monitoring physicochemical properties. This strategy led to the discovery of macrocyclic peptide-peptoid hybrids with high CXCR7 binding affinities (K_i < 100 nM) and measurable passive permeability (P_{app} > 5 x 10^{-6} cm/sec). Moreover, bioactive peptide **25** (K_i = 9 nM) achieved oral bioavailability of 18% in rats, which was commensurate with the observed plasma clearance values upon intravenous administration.

INTRODUCTION

The chemokine receptor CXCR7 is a member of the G-protein coupled receptor (GPCR) family that binds to its chemokine ligands CXCL11 and CXCL12 with high affinity. CXCL12, also known as SDF-1, has many physiological effects including acting as a stimulator of B cell lymphopoiesis and bone marrow myelopoiesis.[1,2] The first identified CXCL12-binding chemokine GPCR was CXCR4, which received a great deal of attention due to its role in the HIV replication cycle, acting as a co-receptor for the entry of HIV into T cells.[3] Further research

has identified pathways activated by CXCR4 including extracellular signal-related kinase and protein kinase B leading to pleiotropic effects.

Unlike CXCR4, CXCR7 signals solely through β-arrestin in response to CXCL12 binding, without noticeable activation of G-protein coupled pathways.[4] Nonetheless, the molecular pharmacology of CXCR7 is complex as it is known to homodimerize as well as heterodimerize with CXCR4, affecting its internalization.[5,6] It has also been reported to act as a scavenging receptor for CXCL12, resulting in the modulation of CXCR4 chemokine axis.[7]

CXCR7 expression is tightly regulated and is enhanced during pathological processes such as cancer and inflammation.[8] It has been shown that CXCR7 plays an essential role in the CXCL12/CXCR4-mediated transendothelial migration of cancer cells.[9] Recently it was reported that CXCR7 modulation ameliorates atherosclerosis and promotes vascular remodeling through increased cholesterol uptake in adipose tissue.[10] CXCR7 has also been shown to act as a decoy receptor for adrenomedullin, a peptide hormone playing a key role in cardiovascular development.[11] A Phase II clinical study evaluated the safety and efficacy of CXCL12 gene therapy in heart failure patients,[12] providing further impetus for the delivery of orally bioavailable CXCR7 ligands that can modulate levels of CXCL12, as an attractive therapeutic drug target.

The identification and development of small molecules for CXCR7 have been described in several publications[13-15] and patent applications.[16-27] Since CXCR4 and CXCR7 share the same chemokine ligand CXCL12, and peptide derivatives for CXCR4 have been successfully developed,[28-31] there is also strong interest in identifying peptides for modulating CXCR7 activity.[32,33] Peptidic macrocycles in particular may provide advantages over small molecules in terms of potency, selectivity, and reduced off-target activity.[34,35]

RESULTS AND DISCUSSION

Compound Synthesis. All peptides were synthesized via standard Fmoc solid phase peptide synthesis methods using the 2-chloro-tritylchloride (CTC) resin.[36] After resin cleavage, the resulting acyclic peptide-peptoid hybrids underwent macrolactamization under dilute solution phase conditions to deliver either the cyclic side-chain protected peptide-peptoids or the final cyclic peptide-peptoids.[37] The cyclic side-chain protected peptide-peptoids were globally deprotected to afford the target compounds. All final compounds were purified using reversed-phase HPLC and analyzed to confirm > 95% purity.

CXCR7 Pharmacology. The binding affinity of peptides (given as K_i value) against CXCR7 was determined by their ability to displace radiolabeled ^{125}I-CXCL12 from membranes obtained from a cell line overexpressing the human CXCR7 receptor.[38] The functional agonist activity of peptides (given as EC_{50} value) against CXCR7 was determined by their ability to induce β-arrestin recruitment in a cell line overexpressing the human CXCR7 receptor.[39]

Passive Cell Permeability and EPSA. The rate of peptides to passively diffuse through cell membranes was determined in a permeability assay using a low-efflux Madin-Darby canine kidney (MDCKII-LE) cell line.[40] To guide the improvement of passive permeability, the polarity of peptides was measured by EPSA, a supercritical fluid chromatography method.[41,42] EPSA values are analogous to calculated polar surface area (e.g. TPSA) values in medicinal chemistry programs. It has been shown that EPSA values of less than 90 are a necessary requirement for peptides to achieve measurable passive permeability.[43] In contrast, while criteria for calculated PSA to achieve oral bioavailability have been described in literature for small molecules (TPSA < 140), consistent guidelines for the prospective design of peptides or macrocycles have not been established.

Macrocyclic hexapeptide **1** (Figure 1) has been reported as a CXCR7 modulator with functional activity in the low nanomolar range.[44] Upon resynthesis its functional activity in the CXCR7 β-arrestin assay was confirmed (EC_{50} = 46 nM), however, the binding affinity against CXCR7 was relatively moderate (K_i = 2.1 μM). Furthermore, due to the presence of a basic arginine moiety, the compound showed poor permeability (P_{app} < 1 x 10^{-6} cm/s) in the MDCKII-LE permeability assay. In this work, we synthesized novel macrocyclic peptide-peptoid hybrids as an alternative to peptide **1**, in order to identify compounds with improved binding affinity and lower overall polarity, with the goal of increasing passive permeability toward the development of orally bioavailable CXCR7 modulators.

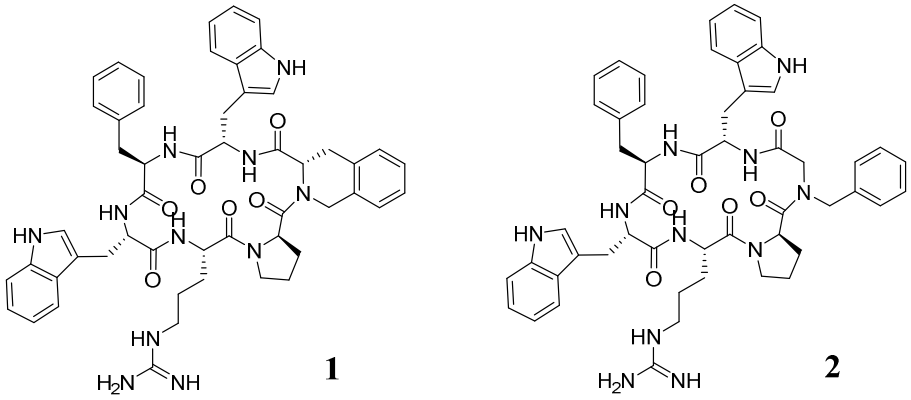

Figure 1. Structures of peptide **1** and peptoid **2**.

To help guide the optimization of binding affinity, a homology model of CXCR7 was developed based on the crystal structure of CXCR4 in complex with a macrocyclic peptide ligand (see Experimental Section).[45] Induced fit docking of peptide **1** provided a hypothesis for its bioactive conformation in the CXCR7 binding pocket (Figure 2) that suggested strategies to improve binding affinity. The proposed docking model shows the tetrahydro-isoquinoline-3-carboxylic acid (TIC) group residing in a large hydrophobic pocket formed by Trp100, Phe124,

Leu128, Trp265, and Leu305, but without a tight contact for the TIC phenyl ring, indicating additional space for enhancing hydrophobic complementarity and improving potency.

The implementation of peptoid residues offers the potential for modular diversification of macrocyclic peptides due to broad availability of synthetic building blocks.[46-48] Peptide to peptoid substitutions have been also shown to improve both metabolic stability and cell permeability.[49] Since the TIC group in **1** contains an N-benzyl substructure, we hypothesized that it could be replaced by an N-linked peptoid residue, allowing the efficient exploration of peptoid side chains at this position using primary amine reagents. This was confirmed by the synthesis of peptide-peptoid hybrid **2** (Figure 1, Table 1) with a binding affinity (K_i = 4.5 μM) comparable to that of peptide **1** (K_i = 2.1 μM).

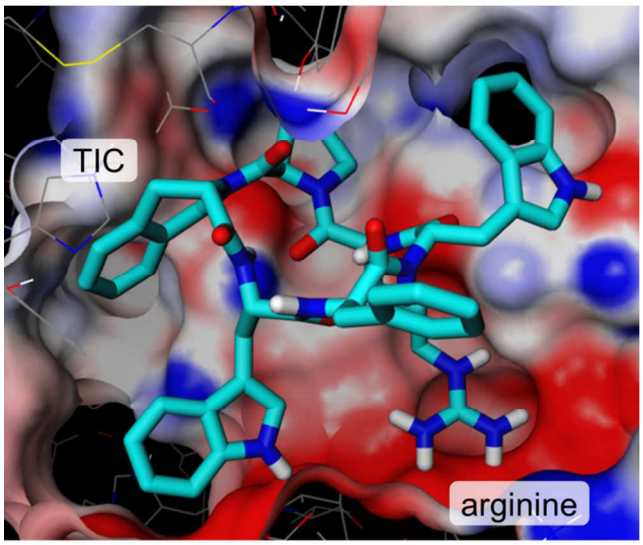

Figure 2. Computational docking of peptide **1** in a homology model of the CXCR7 receptor. The TIC group is located in a large hydrophobic pocket (white) with room for further expansion. The arginine side chain points into a pocket containing acidic residues, forming favorable hydrogen bonding and electrostatic interactions with negatively charged regions (red).

In order to test the hypothesis that the N-benzyl peptoid group binds in a hydrophobic pocket with additional space, a series of analogs with larger side chains at the peptoid position were synthesized, guided in part by docking a larger series of synthetically available building blocks into the CXCR7 receptor homology model (Table 1). Analog **4** with an N-phenylpropyl side chain (K_i = 96 nM) showed a 50-fold improved binding affinity over the shorter N-benzyl (**2**) and N-phenethyl (**3**) moieties. Further elongation of the side chain did not lead to additional affinity gain (data not shown). Optimization of the side chain phenyl ring of **4** with F and Cl substituents further increased affinity by a factor of 15, culminating in **5** and **6** with single-digit nanomolar binding affinities, approximately 750-fold more potent than the initial peptoid **2**. The relative docking scores, expressing free energy of binding, correlated well with the experimental binding affinities (Table 1), which indicates an improved complementary fit of the side chain into the hydrophobic pocket, resulting in an enhanced binding of the peptoids. Notably, one of the most potent analogs (**6**) also showed the best relative docking score in our computational modeling. Albeit not the most potent analog, peptoid **4** was selected as the reference compound for the next set of structural modifications, knowing that the ring substitutions of **5** and **6** could be reintroduced in the final design stage to regain binding affinity.

Table 1. Peptoid variations with improved binding affinity.

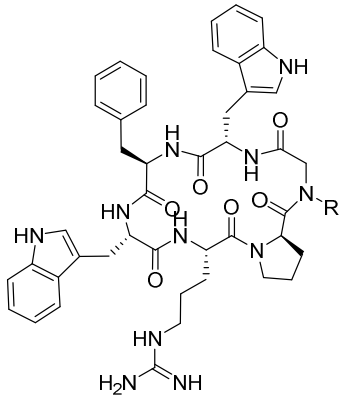

Compd.	R (peptoid)	CXCR7 K_i [nM][a]	Docking Score[b]	ClogP
2	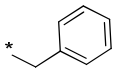	4500 (5.3±0.3)	-14.4	5.2
3	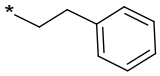	7700 (5.1±0.1)	-14.1	5.7
4	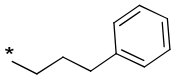	96 (7.0±0.2)	-15.3	6.1
5	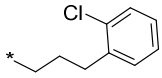	6 (8.3±0.3)	-16.2	6.8
6	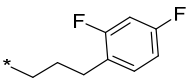	8 (8.1±0.2)	-16.4	6.3

[a]Values were determined by a radioligand binding assay and are reported as geometric mean of at least two independent experiments with pK_i ± SD in parentheses. [b]Glide XP docking score, where more negative values indicate stronger binding affinity (see Experimental Section).

In order to evaluate whether the backbone conformation of the peptide-peptoid hybrid **4** remained unchanged compared to peptide **1**, we employed NMR spectroscopy to gain information on the compound conformation in DMSO. The resulting data showed that **1** and **4** have similar conformations, both with two backbone transannular hydrogen bonds between 1-tryptophan and 4-arginine according to NMR temperature coefficient data (Table S1). The slightly larger $^3J_{NH\text{-}\alpha H}$ value of **4** at 4-arginine (9.1 Hz) indicated that the dihedral angle H-N-C_α-H is closer to 180 degrees. The overall backbone conformation is similar to that of previously reported orally bioavailable macrocyclic peptides,[50,51] indicating the potential for this scaffold to provide reasonable passive cell membrane permeability and oral bioavailability when side chain polarity is limited.

After obtaining peptoid analogs with good binding affinity, we shifted our attention towards improving passive permeability. Our focus was on replacing the arginine side chain, which is positively charged at physiological pH and likely contributes to the poor passive permeability of parent peptide **1**. The EPSA values for peptides **1**-**6** were determined to be in the range of 135

and 150, and not surprisingly, they exhibited poor passive permeability (P_{app} < 1 x 10^{-6} cm/s). The docking model of peptide **1** in the CXCR7 receptor homology model indicated that the arginine side chain points into a polar pocket containing aspartate and glutamate residues, forming favorable hydrogen bonding and electrostatic interactions with Asp275 and Glu290 (Figure 2). We anticipated that replacement of the arginine side chain with non-basic or less polar residues, while retaining binding affinity, would be challenging. Nevertheless, arginine replacements with improved membrane permeability have been described in the literature,[52,53] and we set out to explore the effects of unnatural amino acids containing heterocyclic ring systems (Table 2).

Table 2. Arginine replacements with decreased polarity.

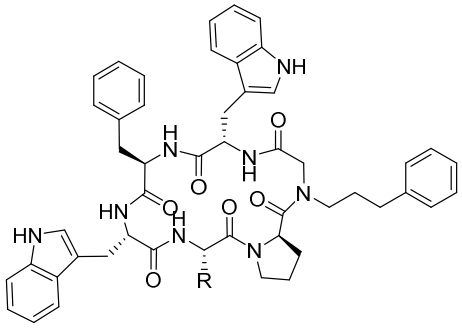

Compd.	R	CXCR7 K_i [nM][a]	EPSA[b]	ClogP
4	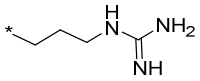	96 (7.0±0.2)	145	6.1
7	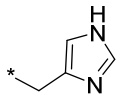	30 (7.5±0.1)	127	6.7
8	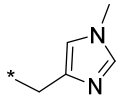	410 (6.4±1.1)	120	6.8
9	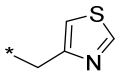	32 (7.5±0.3)	123	7.5
10	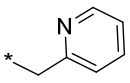	63 (7.2±0.1)	120	7.6

11	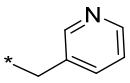	71 (7.1±0.1)	116	7.6
12	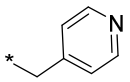	189 (6.7±0.3)	116	7.6
13	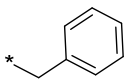	774 (6.1±0.3)	120	9.1

[a]Values were determined by a radioligand binding assay and are reported as geometric mean of at least two independent experiments with pK_i ± SD in parentheses. [b]Values were measured by a chromatographic method.[41,43]

Replacing the arginine side chain of **4** with various five- and six-membered heteroaryl rings led to a pronounced decrease in polarity, with EPSA values ranging from 116 to 127 for peptoid analogs **7**-**12**, approximately 20-30 units lower than that of **4** (EPSA = 145). Encouragingly, several arginine replacements (**7**, **9**-**11**) were equipotent or showed an even greater binding affinity compared to **4**. To explore the lowest achievable polarity for this side chain we also prepared a non-heteroaryl phenylalanine analog **13** which had an EPSA value similar to those of analogs **7**-**12**. However, presumably due to the lack of functional groups capable of hydrogen bonding or electrostatic interactions with the negatively charged regions in the binding pocket (Figure 2), its binding affinity decreased 8-fold compared to **4**. Since peptoid **11** exhibited the best balance of good potency, matching that of **4**, and low polarity (EPSA = 116), it was selected as a starting point for further structural optimization.

After successful replacement of the arginine side chain with heterocyclic ring systems, we tested the effect of replacing the two tryptophan residues with alternate aryl side chains (Table 3). Substitution of one tryptophan residue in **11** by hhPhe resulted in **14** that showed an EPSA decrease from 116 to 104, but permeability in the MDCKII-LE assay remained low (P_{app} = 0.9 x 10^{-6} cm/s). Additional replacement of the second tryptophan residue with hhPhe (**15**) and hPhe (**16**) further reduced EPSA below the aforementioned threshold of less than 90, resulting for the first time in measurable passive permeability (P_{app} > 1 x 10^{-6} cm/s). Since **15** and **16** had slightly

reduced binding affinity, we were particularly intrigued by peptoid **18** with a non-aromatic t-butyl substitution, which retained the binding affinity of the tryptophan analog (**14**). With its further reduced polarity (EPSA = 79), **18** also exhibited the highest passive permeability (P_{app} = 4.8 x 10^{-6} cm/s) measured thus far in this series. Interestingly, a comparably low EPSA value for the equipotent peptoid **17** did not translate to measurable permeability (P_{app} = 0.7 x 10^{-6} cm/s).

Table 3. Tryptophan substitutions with reduced polarity and increased passive permeability.

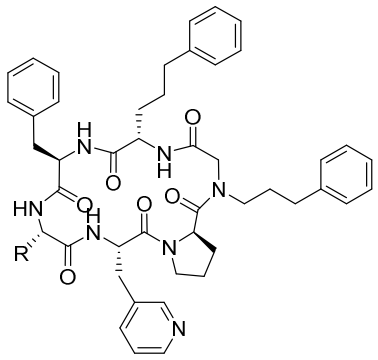

Compd.	R	CXCR7 K_i [nM][a]	EPSA[b]	ClogP	P_{app} [10^{-6} cm/s][c]
14	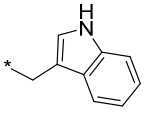	23 (7.6±0.2)	104	8.7	0.9
15	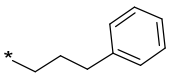	71 (7.2±0.2)	90	9.8	1.2
16	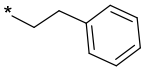	88 (7.1±0.3)	89	9.3	1.8
17	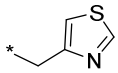	24 (7.6±0.1)	89	7.1	0.7
18	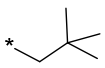	34 (7.5±0.1)	79	9.2	4.8

[a]Values were determined by a radioligand binding assay and are reported as geometric mean of at least two independent experiments with pK_i ± SD in parentheses. [b]Values were measured by a chromatographic method.[41,43] [c]Values were determined by a permeability assay in a low-efflux Madin-Darby canine kidney cell line.[40]

With **18** emerging as the most promising analog, we embarked on further optimization of various side chains to obtain peptides with an improved balance between potency and passive permeability (Table 4). First, at the original arginine position, we replaced the 3-pyridyl group with a thiazole ring for which we expected a modest potency boost from known SAR (Table 2). This was confirmed with peptide **19** (K_i = 9 nM). The pyridyl to thiazole substitution resulted only in a negligible change in EPSA and permeability. In the next step, shortening of the side chain from hhPhe (**19**) to phenylalanine (**20**) improved permeability (P_{app} = 6.6 x 10^{-6} cm/s) but potency was decreased by 50-fold. Again taking advantage of existing SAR (Table 1), we anticipated a potency boost by switching to a 2,4-difluoro-substituted N-phenylpropyl side chain at the peptoid position. Indeed, **21** showed a 20-fold increase in potency (K_i = 25 nM) in comparison to **20**. The introduction of an additional 4-fluoro substituent on the phenylalanine side chain (**22**) further increased permeability (P_{app} = 7.6 x 10^{-6} cm/s). In an attempt to eliminate another aromatic group from the peptide, we also investigated aliphatic side chains (**23**, **24**). Interestingly, the introduction of a second t-butyl group in **24** showed the highest measured permeability in this series (P_{app} = 8.3 x 10^{-6} cm/s). Peptide **25**, however, provided the best overall balance between potency (K_i = 9 nM) and passive permeability (P_{app} = 6.2 x 10^{-6} cm/s), and was progressed towards examination of its *in vivo* oral absorption potential in rats. Measured in the CXCR7 β-arrestin functional assay, the activity of **25** (EC_{50} = 15 nM) showed a 3-fold improvement over the initial peptide **1** (EC_{50} = 46 nM).

Table 4. Side chain optimization with improved balance between potency and permeability.

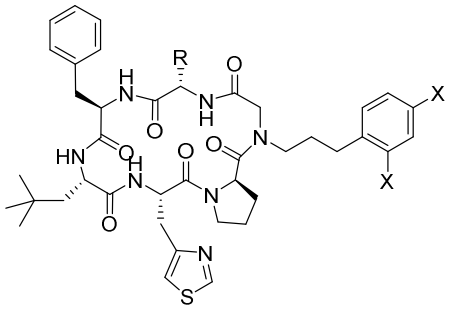

Compd.	R	X	CXCR7 K_i [nM][a]	EPSA[b]	ClogP	P_{app} [10^{-6} cm/s][c]
19	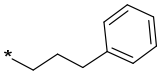	H	9 (8.1±0.1)	80	9.0	4.0
20	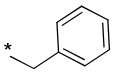	H	537 (6.3±0.1)	79	7.9	6.6
21	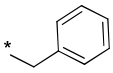	F	25 (7.6±0.1)	74	8.2	5.2
22	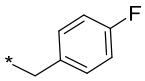	F	42 (7.4±0.1)	74	8.4	7.6
23	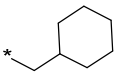	F	34 (7.5±0.1)	74	9.5	3.8
24		F	95 (7.0±0.1)	70	8.7	8.3
25	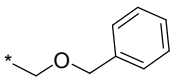	F	9 (8.0±0.4)	77	8.3	6.2

[a]Values were determined by a radioligand binding assay and are reported as geometric mean of at least two independent experiments with pK_i ± SD in parentheses. [b]Values were measured by a chromatographic method.[41,43] [c]Values were determined by a permeability assay in a low-efflux Madin-Darby canine kidney cell line.[40]

To summarize, our design strategy was to employ peptoids capable of probing a larger diversity of side chains to efficiently explore a large hydrophobic pocket in the CXCR7 binding site. Simultaneously, we monitored physicochemical properties such as polarity measured by EPSA, with the aim of identifying peptide-peptoid hybrids that were both potent and passively permeable across cell membranes. The overall progression of peptides synthesized in these iterative design cycles is shown in Figure 3. The initial peptides showed only weak binding

affinity and high polarity with no measurable permeability. In the first design step, implementation of N-linked peptoids led to peptide-peptoid hybrids with improved binding affinity, but relatively high EPSA values (Table 1). Next, replacement of the basic arginine side chain yielded compounds with lower polarity while retaining moderate activity (Table 2). Substitution of the two tryptophan residues yielded analogs with further reduced polarity (Table 3), and ultimately resulted in peptides with improved potency and passive permeability (Table 4).

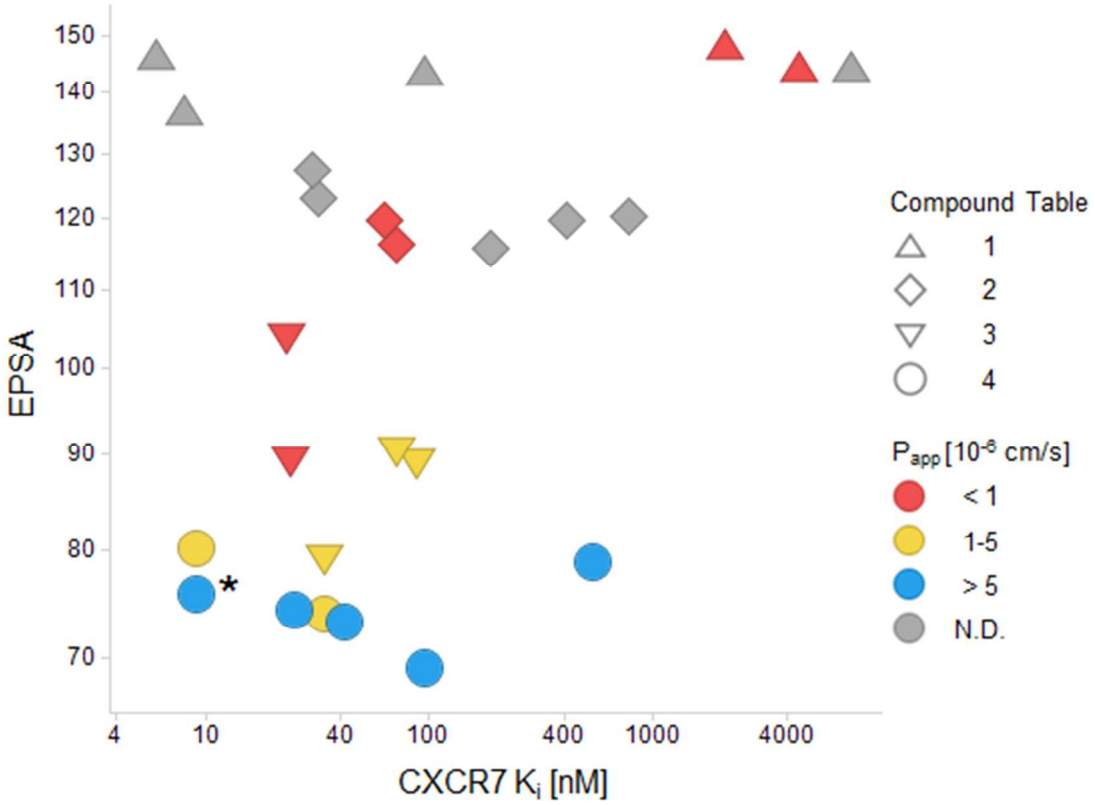

Figure 3. Optimization of peptides **1-25** as measured by binding affinity (CXCR7 K_i), polarity (EPSA), and *in vitro* passive permeability (P_{app}). Compounds exemplified in Tables 1-4 are grouped by shape. Permeability values of peptides were binned and are highlighted by color. Peptide **25** (*) was selected for further characterization.

The peptides described herein are only a subset of a larger collection of analogs that were synthesized and tested during the iterative design cycle process. Having a large data set of related analogs with experimental data in hand, we were interested to learn of any relationships between physicochemical properties and experimental data to guide prospective peptide design efforts. The correlation between passive permeability (P_{app}), polarity (EPSA), and lipophilicity (ClogP) is shown in Figure 4. In agreement with previous findings,[43] our data confirms that EPSA values of less than 90 are indeed necessary for peptides to achieve measurable passive permeability. However, satisfying this rule alone did not always result in permeable peptides (Figure 4, left). Our data suggests that peptides also need to fulfill a certain lipophilicity requirement, and with this particular scaffold they must have ClogP values between 7.5 and 10 in order to yield measureable passive permeability. Peptides outside this ClogP range did not lead to substantial permeability in the MDCKII-LE assay (Figure 4, right). Apparently, not only is high polarity detrimental to passive permeability, but high lipophilicity seems to impede passive perfusion through the membrane. Similar findings of a parabolic correlation between a variety of calculated logP and experimental P_{app} values were observed by other groups as well, claiming 'islands of permeability' where only peptides with the right balance of polarity, lipophilicity and solubility are likely to have measurable permeability.[54,55] The equivalent analysis correlating passive permeability with calculated PSA (TPSA) instead of EPSA revealed that the cutoff criteria established in literature (TPSA < 140) would have not been applicable for this series of macrocyclic peptides in a prospective design (Figure S1).

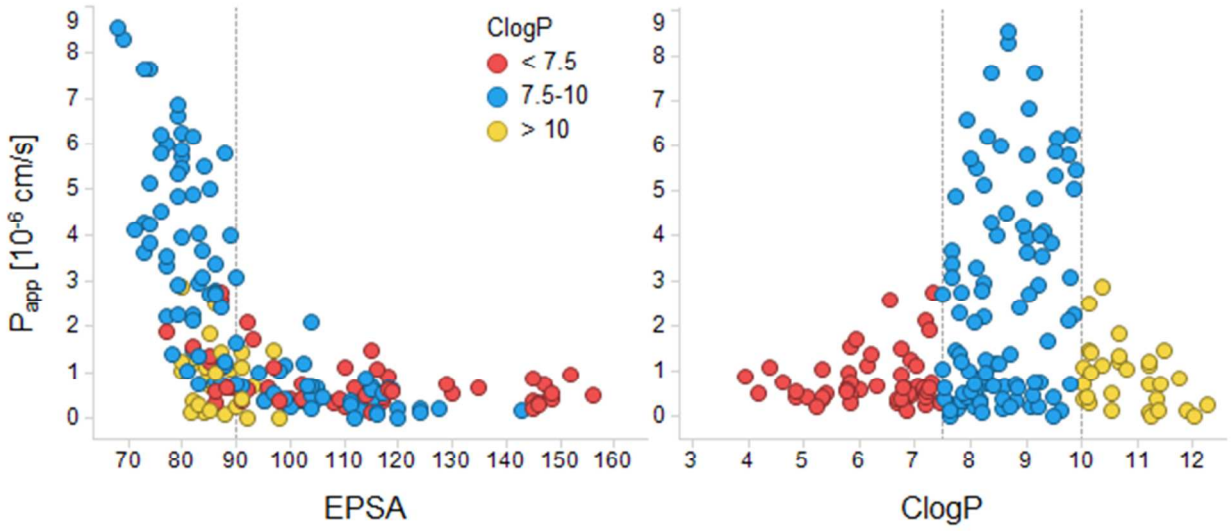

Figure 4. Correlation between passive permeability (P_{app}), polarity (EPSA) and lipophilicity (ClogP). Dashed lines indicate the EPSA threshold of less than 90 and a ClogP range from 7.5 to 10, necessary to achieve measurable permeability for peptides with this particular scaffold.

In addition to the optimization of side chains, N-methylation of backbone amide groups has been shown to have a beneficial effect on permeability in cyclic peptide scaffolds.[51,56-60] We examined the effect of N-methylation on selected peptides developed in this study (Table 5). We focused mainly on N-methylation of the R_2 and R_3 backbone amides since analogs methylated at these positions are expected to have a similar low-dielectric backbone conformation compared to cyclic peptides that were previously shown to have good permeability.[48,55] We found that N-methylation was generally beneficial to permeability when ClogP was in a favorable range, as described above. For example, peptide **17** (Table 3) had shown poor permeability (P_{app} = 0.7 x 10^{-6} cm/s) despite its low polarity value (EPSA = 89). The likely reason for that is the ClogP value of 7.1 which is below the optimal range of 7.5 and 10 (Figure 4). N-methylation of the R_3 (**26**) and R_2/R_3 (**27**) backbone amides not only further decreased polarity (EPSA = 86 and 83, respectively), but also slightly raised the ClogP values (ClogP = 7.8 and 8.5, respectively)

towards the optimal range necessary to achieve passive permeability. As a result (Table 5), we improved the low permeability of **17** with both its mono-N-methyl derivative **26** (P_{app} > 2.7 x 10^{-6} cm/s) and bis-N-methyl derivative **27** (P_{app} = 4.0 x 10^{-6} cm/s). Ultimately, we decided not to pursue the N-methylation strategy further, because in most cases N-methylation at the R_2 position also had a deleterious effect on CXCR7 binding affinity.

Table 5. N-methylation of cyclic peptide scaffold to improve permeability.

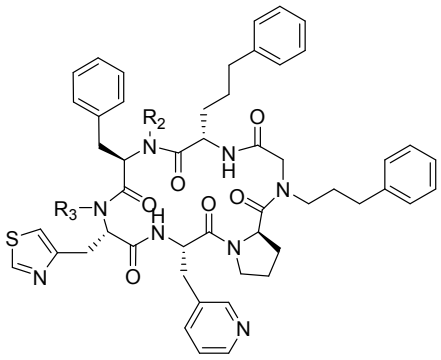

Compd.	R_2	R_3	CXCR7 K_i [nM][a]	EPSA[b]	ClogP	P_{app} [10^{-6} cm/s][c]
17	H	H	24 (7.6±0.1)	89	7.1	0.7
26	H	Me	20 (7.7±0.3)	86	7.8	2.7
27	Me	Me	211 (6.7±0.2)	83	8.5	4.0

[a]Values were determined by a radioligand binding assay and are reported as geometric mean of at least two independent experiments with pK_i ± SD in parentheses. [b]Values were measured by a chromatographic method.[41,43] [c]Values were determined by a permeability assay in a low-efflux Madin-Darby canine kidney cell line.[40]

To assess whether oral bioavailability can be achieved for peptides with measurable passive permeability as determined in the MDCKII-LE assay, the pharmacokinetics of **25** was examined in rats. The intravenous (IV) and oral (PO) pharmacokinetic results are shown in Table 6. After IV dosing, peptide **25** exhibited a high plasma clearance (CL_p) that exceeded the rat hepatic blood flow value (70 mL/min/kg).[61] Consistent with this observation, incubation of **25** (1 μM) with NADPH-supplemented rat liver microsomes resulted in facile metabolic turnover leading to

a short half-life (45 min) and a high apparent intrinsic clearance value (610 μL/min/mg). The finding that **25** was resistant towards metabolism (half-life > 2 h) in rat liver microsomes lacking NADPH cofactor strongly suggests a role for rat cytochrome P450 enzymes in the oxidative metabolism of **25** as a cause of its metabolic instability, which leads to observed high *in vivo* plasma clearance. The volume of distribution ($V_{d,ss}$) for **25** was considerably above the total body water volume (0.6 L/kg) indicating extensive distribution into tissues. The corresponding half-life after IV administration was relatively short (< 1 h).

Table 6. Pharmacokinetic profile of compound **25** in rats[a].

Compd.	CL_p[b] [mL/min/kg]	$V_{d,ss}$[b] [L/kg]	$t_{1/2}$[b] [h]	AUC[b] [ng/mL×h]	C_{max}[c] [ng/mL]	AUC[c] [ng/mL×h]	F [%]	$f_{u,p}$
25	136±9	4.4±0.3	0.95±0.01	124±9	97±18	224±30	18	0.011

[a]Pharmacokinetic parameters were calculated from plasma concentration-time data in male Wistar Han rats (2 animals per route) and are reported as mean ± SD values. [b]Following IV administration (1 mg/kg) formulated in DMSO: Cremophor: Saline (5:5:90 v/v). [c]Following PO administration (10 mg/kg) as an emulsion in 10% Miglyol 812: Cremophor RH40: Capmul MCM (30:40:30 v/v) and 90% water (SEDDS formulation).

Following PO administration of **25** in the lipophilic self-emulsifying drug delivery system (SEDDS) formulation at 10 mg/kg, the systemic exposure measured by maximal plasma concentrations (C_{max}) and area under the plasma concentration-time curve (AUC) was 97 ng/mL and 224 ng/mL x h, respectively. The corresponding oral bioavailability (F) of **25** was 18%. The reason for achieving oral systemic exposure despite the hepatic blood flow-limited intrinsic clearance of **25** remains unclear at the present time. One possibility is the saturation of first-pass metabolic extraction by rat cytochrome P450 enzymes in the small intestine and the liver[62] due to the 10-fold higher PO dose administered relative to the IV dose.

When normalized against the rat plasma unbound fraction ($f_{u,p}$),[63] the free C_{max} value (~ 1.3 nM) of **25** after PO dosing was approximately 7-fold lower than the corresponding CXCR7

binding affinity (9 nM). In order to probe *in vivo* CXCR7 pharmacology, sustained unbound plasma concentrations several fold over the K_i value are desired, which currently would be unattainable with a reasonable PO dosing regimen of **25**.

CONCLUSION

In this study, we demonstrated the successful optimization of low affinity, highly polar and non-permeable peptides towards macrocyclic peptide-peptoid hybrids with improved CXCR7 binding affinity (K_i < 100 nM) and *in vitro* passive permeability in the MDCKII-LE assay (P_{app} > 5 x 10^{-6} cm/sec), thereby achieving our goal to identify potent and cell-permeable CXCR7 modulators. Moreover, bioactive peptide **25** (K_i = 9 nM, EC_{50} = 15 nM) with measurable passive permeability (P_{app} = 6.2 x 10^{-6} cm/sec) also demonstrated reasonable oral bioavailability in rats (F = 18%). A pragmatic next step to further increase the oral absorption of **25** would be to improve its metabolic stability whilst maintaining CXCR7 potency and the favorable passive permeability characteristics.

EXPERIMENTAL SECTION

All procedures performed on animals in this study were in accordance with established guidelines and regulations, and were reviewed and approved by Pfizer Institutional Animal Care and Use Committee. Pfizer animal care facilities that supported this work are fully accredited by AAALAC International.

Peptide Synthesis. Standard solid phase peptide synthesis (SPPS) was used to synthesize the peptide-peptoid hybrids. Unless otherwise stated, the resin (100-200 mesh or 200-400 mesh, cross linking degree: 1% DVB), Fmoc amino acids, and other starting materials were commercially available and used without further purification. After cleaving from the resin, the

resulting acyclic peptides were then cyclized under dilute solution phase conditions: (a) BOP, HOBt, DIPEA, DCM ([substrate] ~6 mM), 16 h, and (b) EDC, HOAt, DIPEA, ACN:DCM (1:1, 0.5 mg of linear peptide-peptoid compound/mL), 16 h. Full synthetic details for individual peptide-peptoid hybrids are provided in the Supporting Information.

Purification of Peptides. Crude material was dissolved in a minimal amount of water and purified using multiple conditions: (a) Waters 4000 system connected to a Phenomenex Luna™ C18, reversed phase HPLC column (10 microns, 100 Å, 25 mm x 200 mm) eluting with a solvent gradient A:B where A = 0.1% TFA in water and B = 0.1% TFA in ACN:water (4:1), (b) Shimadzu LC-8A preparative HPLC system coupled to a Higgins C18 analytical column (5 microns, 100 Å, 20 mm x 250 mm) eluting with 0.1% TFA in water:0.1% TFA in ACN (40:60 to 0:100) over 30 min at a flow rate of 10 mL/min, (c) Shimadzu LC-8A preparative HPLC system coupled to a Higgins C18 analytical column (5 micron, 100 Å, 20 mm x 250 mm) eluting with 0.1% TFA in water:0.1% TFA in ACN (10:90 to 0:100) over 30 min at a flow rate of 10 mL/min, and (d) Waters system coupled to a SunFire C18 column (5 microns, 100 Å, 19 mm x 100 mm) eluting with 0.05% TFA in water:0.05% TFA in ACN (90:10 to 50:50 for 10.5 min, then 50:50 to 0:100 for 0.5 min, then 5:95 for 1 min) at a flow rate of 25 mL/min. Specific conditions for individual peptide-peptoid hybrids are provided in the Supporting Information.

Purity Analysis of Peptides. Purified material was analyzed to confirm > 95% purity under a variety of conditions: (a) HP1090 system coupled to a Phenomenex C18 (2) (5 microns, 100 Å, 4.6 mm x 150 mm) reversed phase HPLC column eluting with a solvent gradient of A:C, where A = 0.1% TFA in water and C = 0.09% TFA in ACN:water (4:1) over 20 minutes at a flow rate of 1.0 mL/min, (b) Waters LC/MS/ELSD (single quad MS) system coupled to an Acquity HSS T3 UPLC reversed phase column (1.8 microns, 100 Å, 2.1 x 50 mm) eluting with 0.05% TFA in

water: 0.05% TFA in ACN (95:5 to 0:100 over 5 min then 0:100 for 2.5 min) at flow rate of 0.7 mL/min, and (c) Pure peptides were analyzed using a Waters LC/MS/ELSD (single quad MS) system coupled to a SunFire C18 column (5 microns, 100 Å, 4.6 mm x 50 mm) reversed phase column eluting with 0.05% TFA in water:0.05% TFA in ACN (90:10 to 50:50 for 3.75 min, then 50:50 to 5:95 for 0.5 min, then 5:95 for 0.5 min) at a flow rate of 2.0 mL/min. Specific conditions, retention times, and UV purities (215 nm or 220 nm) for individual peptide-peptoid hybrids are provided in the Supporting Information.

CXCR7 radiolabeled ligand binding assay. The binding affinity of test compounds for the human CXCR7 chemokine receptor was determined by their ability to displace ^{125}I-CXCL12 (Perkin Elmer) from membranes obtained from CHO-K1 cells overexpressing the human CXCR7 receptor (DiscoveRx). K_i values are reported as the geometric mean of at least two independent experiments each of which was run in duplicate.

Test compounds were serialized in 100% DMSO and spotted into 96 well plates (NBS). Total binding wells were spotted with diluent. Non-specific wells were defined by the addition of potent CXCR7 agonist. 10 μL of ^{125}I-CXCL12 with a final concentration of 100 pM was added to each well of the plate, followed by the addition of 90 μL of membranes. Both the membranes and ^{125}I-CXCL12 were diluted to the appropriate concentration in assay buffer (HBSS containing 10 mM HEPES and 0.2% BSA). After the addition membranes plates were incubated at room temperature for 2 h (shaking). Reactions were terminated by rapid filtration through poly(ethyleneimine) (0.3%) treated 96 well GF/C Unifilter plates (Perkin Elmer). Unbound ligand was removed by washing the filters with ice cold wash buffer. Filters were allowed to dry thoroughly prior to the addition of Ready Safe scintillation fluid (Perkin Elmer). The amount of bound ^{125}I-CXCL12 was quantitated by reading plates on the Trilux (Perkin Elmer).

CXCR7 β-arrestin functional assay. The agonist activity of test compounds was determined by their ability to induce β-arrestin recruitment in CHO-K1 cells overexpressing the human CXCR7 receptor (DiscoveRx). EC_{50} values are reported as the geometric mean of at least two independent experiments each of which was run in duplicate.

The receptor is fused with the small enzyme fragment ProLink™ and co-expressed in the cells stably expressing a fusion protein of β-arrestin and the larger, N-terminal deletion mutant of β-gal (called enzyme acceptor or EA). Agonist activation of the receptor by test compounds causes binding of β-arrestin (EA) to the ProLink-tagged CXCR7 resulting in the formation of active β-gal enzyme. Enzyme activity is measured using chemiluminescent PathHunter® detection reagents (DiscoveRx).

Prior to the assay, cells are removed from culture flasks and plated at a density of 6K viable cells per well in white solid bottom 384 well plates. After the addition of cells, plates were placed in humidified 37 ℃ 5% CO_2 incubator for 18-24 h. Test compounds were serialized in 100% DMSO and diluted in assay buffer (HBSS containing 10 mM HEPES and 0.1% BSA) prior to their addition to the cell plates. Media was removed from the cell plates and 20 μL of compound or diluent was added to the appropriate wells of the plate. Following compound addition, cell plates were incubated at 37 ℃ in 5% CO_2 for 30 min. After incubation 20 μL of PathHunter® detection reagents (DiscoveRx) were added to each well of the plate. Plates were incubated at 23 ℃ in the dark for 1 h prior to reading on the Envision (Perkin Elmer).

MDCKII-LE Permeability Assay. Passive permeability was determined using a low-efflux Madin-Darby canine kidney (MDCKII-LE) cell line (Pfizer, Groton, CT). Cells were grown in minimum essential medium α-nucleosides (Life Technologies, Grand Island, NY) supplemented with 10% fetal bovine serum, 1% minimum non-essential amino acids solution, 1%

GlutaMAX™ and 1% penicillin-streptomycin prior to seeding into Millipore 96-well cell culture insert plates (EMD Millipore Corporation). MDCKII-LE cells were cultured on the inserts with 100 µL medium per well on the apical side and 36 mL for all 96 wells on the basolateral side. Donor solutions were prepared from HBSS containing 20 mM HEPES, pH 6.5. Stock solutions of test compounds, prepared at 5 mM in DMSO, were used to prepare donor solutions of 6 µM compound. Receiver solutions were prepared from HBSS containing 20 mM HEPES and 0.4 % BSA (w/v), pH 7.4. Prior to the assay, cell culture medium was removed and cells were pre-incubated with HBSS for 10 min. To start the assay, 100 µL of donor solution and 300 µL of receiver solution were added to the apical and basolateral chambers, respectively. After 90 min incubations, aliquots were taken from the receiver chambers to determine the translocated amount of compound. Samples were taken from the donor chambers before and after incubation to determine the initial concentration (C_0) and recovery values. An internal standard solution, 0.5 µg/mL CP-628374 (MW = 687) in 100% methanol, was added to the receiver and donor samples. The samples were analyzed by LC-MS/MS to determine the peak area for test compound and the internal standard. All incubations were conducted in triplicate.

Apparent permeability values (P_{app}) were calculated according to the following equation:

$$Papp = \frac{dx/dt}{C_0 \times A}$$

where dx is the amount of compound in the receiver compartment, dt is the incubation time, C_0 is the initial concentration in the donor compartment, and A is the area of the filter of the transwell plate.

Pharmacokinetics. Rat pharmacokinetics were determined in male Wistar Han rats sourced from Charles River, weighing between 250-281 g, (n=2/route) following single IV bolus (1

mg/kg) and PO (10 mg/kg) administration. For the IV dose, **25** was formulated in DMSO: Cremophor: Saline (5:5:90 v/v) and administered at 2 mL/kg via the jugular vein cannula. In order to avoid poor aqueous solubility confounding oral bioavailability determination, the PO doses of **25** were administered in a self-emulsifying (SEDDS) formulation. Peptide **25** was presented as an emulsion in 10% Miglyol 812: Cremophor RH40: Capmul MCM (30:40:30 v/v) and 90% water (10 mL/kg). Doses were administered by gavage tube. At 2 min (IV only), 5 min, 15 min, 30 min, 1 h, 2 h, 4 h, 7 h and 24 h post dose, blood samples were taken from previously implanted in-dwelling carotid artery catheters. Blood was centrifuged to produce plasma which was stored frozen until bioanalysis. Bioanalysis of plasma samples was completed using specific HPLC-MS/MS methods with lower limits of detection for **25** equal to or below 1 ng/mL. Pharmacokinetic parameters were calculated using standard non-compartmental analysis.

Molecular Modeling. The crystal structure of CXCR4 in complex with the cyclic peptide antagonist CVX15 (PDB code 3OE0) was used to develop a CXCR7 homology model. The protein sequence of CXCR7 was aligned to the CXCR4 structure using ClustalW. The homology model of CXCR7 was generated using Prime version 3.1 from Schrödinger. Conformational modeling of cyclic peptides was performed using PLOP with robust backbone sampling, and the predicted conformations were used as input for subsequent docking calculations. Docking of compounds into the CXCR7 homology model was conducted using Glide XP from Schrödinger (release 2016-2). The Induced Fit Docking (IFD) protocol, which uses Prime and Glide to induce adjustments in the receptor structure, was employed to investigate binding models of key compounds, such as peptide **1** as well as peptide-peptoid hybrids **2** and **4**. To support optimization of the peptoid position for CXCR7 binding, CombiGlide from Schrödinger was utilized to enumerate virtual libraries of peptide-peptoid hybrids based on commercially

available primary amines and to dock against the CXCR7 homology model to identify peptoid substitutions favorable for binding.

ASSOCIATED CONTENT

Supporting Information. The Supporting Information is available free of charge on the ACS Publication website at DOI:

NMR temperature coefficients and chemical shifts of NHs, $^{3}J_{NH\text{-}\alpha H}$ couplings; EPSA method; correlation plot of passive permeability vs. TPSA; synthetic procedures and analytical data of peptides **1-27**; IV and oral PK concentration vs. time curves for peptide **25** (PDF)

Atomic coordinates of the CXCR7 homology model with computational docking of peptide **1** (PDB)

AUTHOR INFORMATION

Corresponding Authors

*Phone: +1 617 551 3517. E-mail: elnaz.menhaji-klotz@pfizer.com. *Phone: +1 831 459 1307. E-mail: slokey@ucsc.edu. *Phone: +1 650 392 0363. E-mail: davidjearp@circlepharma.com.

Present Addresses

‡B.R.H.: Middletown, Connecticut 06457. ‡M.J.S.: Niantic, Connecticut 06357. ‡J.Y.: MassBiologics, Boston, Massachusetts 02124. #R.T.: Monterey Peninsula College, Monterey, California 93940.

Author Contributions

All authors have given approval to the final version of the manuscript.

Notes

The authors declare the following competing financial interest: M.P.J. and R.S.L. are co-founders of, and advisors to, Circle Pharma and each holds an equity interest in the company.

ACKNOWLEDGMENT

We thank the Chinese Peptide Company for peptide synthesis support.

ABBREVIATIONS USED

CXCR7, CXC chemokine receptor 7; CXCR4, CXC chemokine receptor 4; CXCL12, CXC chemokine ligand 12; EC_{50}, half maximal effective concentration; ELSD, evaporative light scattering detector; HBSS, Hanks' balanced salt solution; HPLC, high-performance liquid chromatography; IV, intravenous; K_i, binding affinity; MDCKII-LE, low-efflux Madin-Darby Canine Kidney cell line; MS, mass spectrometry; NMR, nuclear magnetic resonance; P_{app}, absorptive permeability; PO, oral; SAR, structure-activity relationship; SEDDS, self-emulsifying drug delivery system; UPLC, ultra-performance liquid chromatography; UV, ultraviolet; ACN, acetonitrile; DCM, dichloromethane; DMSO, dimethyl sulfoxide; Fmoc, fluorenylmethyloxycarbonyl; hPhe, homophenylalanine; hhPhe, homohomophenylalanine; TFA, trifluoroacetic acid; TIC, tetrahydroisoquinoline-3-carboxylic acid.

REFERENCES

(1) Nagasawa, T.; Hirota, S.; Tachibana, K.; Takakura, N.; Nishikawa, S.; Kitamura, Y.; Yoshida, N.; Kikutani, H.; Kishimoto, T. Defects of B-cell lymphopoiesis and bone-marrow myelopoiesis in mice lacking the CXC chemokine PBSF/SDF-1. *Nature* **1996,** *382* (6592), 635-638.

(2) Ma, Q.; Jones, D.; Borghesani, P. R.; Segal, R. A.; Nagasawa, T.; Kishimoto, T.; Bronson, R. T.; Springer, T. A. Impaired B-lymphopoiesis, myelopoiesis, and derailed cerebellar neuron

migration in CXCR4- and SDF-1-deficient mice. *Proc. Natl. Acad. Sci. U. S. A.* **1998,** *95* (16), 9448-9453.

(3) Bleul, C. C.; Wu, L.; Hoxie, J. A.; Springer, T. A.; Mackay, C. R. The HIV coreceptors CXCR4 and CCR5 are differentially expressed and regulated on human T lymphocytes. *Proc. Natl. Acad. Sci. U. S. A.* **1997,** *94* (5), 1925-1930.

(4) Rajagopal, S.; Kim, J.; Ahn, S.; Craig, S.; Lam, C. M.; Gerard, N. P.; Gerard, C.; Lefkowitz, R. J. Beta-arrestin- but not G protein-mediated signaling by the "decoy" receptor CXCR7. *Proc. Natl. Acad. Sci. U. S. A.* **2010,** *107* (2), 628-632.

(5) Levoye, A.; Balabanian, K.; Baleux, F.; Bachelerie, F.; Lagane, B. CXCR7 heterodimerizes with CXCR4 and regulates CXCL12-mediated G protein signaling. *Blood* **2009,** *113* (24), 6085-6093.

(6) Sanchez-Alcaniz, J. A.; Haege, S.; Mueller, W.; Pla, R.; Mackay, F.; Schulz, S.; Lopez-Bendito, G.; Stumm, R.; Marin, O. Cxcr7 controls neuronal migration by regulating chemokine responsiveness. *Neuron* **2011,** *69* (1), 77-90.

(7) Naumann, U.; Cameroni, E.; Pruenster, M.; Mahabaleshwar, H.; Raz, E.; Zerwes, H. G.; Rot, A.; Thelen, M. CXCR7 functions as a scavenger for CXCL12 and CXCL11. *PLoS One* **2010,** *5* (2), e9175.

(8) Sanchez-Martin, L.; Sanchez-Mateos, P.; Cabanas, C. CXCR7 impact on CXCL12 biology and disease. *Trends Mol. Med.* **2013,** *19* (1), 12-22.

(9) Zabel, B. A.; Lewen, S.; Berahovich, R. D.; Jaen, J. C.; Schall, T. J. The novel chemokine receptor CXCR7 regulates trans-endothelial migration of cancer cells. *Mol. Cancer* **2011,** *10*, 73.

(10) Li, X.; Zhu, M.; Penfold, M. E.; Koenen, R. R.; Thiemann, A.; Heyll, K.; Akhtar, S.; Koyadan, S.; Wu, Z.; Gremse, F.; Kiessling, F.; van Zandvoort, M.; Schall, T. J.; Weber, C.; Schober, A. Activation of CXCR7 limits atherosclerosis and improves hyperlipidemia by increasing cholesterol uptake in adipose tissue. *Circulation* **2014,** *129* (11), 1244-1253.

(11) Klein, K. R.; Karpinich, N. O.; Espenschied, S. T.; Willcockson, H. H.; Dunworth, W. P.; Hoopes, S. L.; Kushner, E. J.; Bautch, V. L.; Caron, K. M. Decoy receptor CXCR7 modulates adrenomedullin-mediated cardiac and lymphatic vascular development. *Dev. Cell* **2014,** *30* (5), 528-540.

(12) Chung, E. S.; Miller, L.; Patel, A. N.; Anderson, R. D.; Mendelsohn, F. O.; Traverse, J.; Silver, K. H.; Shin, J.; Ewald, G.; Farr, M. J.; Anwaruddin, S.; Plat, F.; Fisher, S. J.; AuWerter, A. T.; Pastore, J. M.; Aras, R.; Penn, M. S. Changes in ventricular remodelling and clinical status during the year following a single administration of stromal cell-derived factor-1 non-viral gene therapy in chronic ischaemic heart failure patients: the STOP-HF randomized Phase II trial. *Eur. Heart J.* **2015,** *36* (33), 2228-2238.

(13) Wijtmans, M.; Maussang, D.; Sirci, F.; Scholten, D. J.; Canals, M.; Mujic-Delic, A.; Chong, M.; Chatalic, K. L.; Custers, H.; Janssen, E.; de Graaf, C.; Smit, M. J.; de Esch, I. J.; Leurs, R. Synthesis, modeling and functional activity of substituted styrene-amides as small-molecule CXCR7 agonists. *Eur. J. Med. Chem.* **2012,** *51*, 184-192.

(14) Uto-Konomi, A.; McKibben, B.; Wirtz, J.; Sato, Y.; Takano, A.; Nanki, T.; Suzuki, S. CXCR7 agonists inhibit the function of CXCL12 by down-regulation of CXCR4. *Biochem. Biophys. Res. Commun.* **2013,** *431* (4), 772-776.

(15) Yoshikawa, Y.; Oishi, S.; Kubo, T.; Tanahara, N.; Fujii, N.; Furuya, T. Optimized method of G-protein-coupled receptor homology modeling: its application to the discovery of novel CXCR7 ligands. *J. Med. Chem.* **2013,** *56* (11), 4236-4251.

(16) Melikian, A.; Burns, J.; McMaster, B. E.; Schall, T.; Wright, J. J. Preparation of Inhibitors of Human Tumor-Expressed CCXCKR2 for the Treatment of Cancer. WO2004058705, 2004.

(17) Burns, J.; Summers, B.; Wang, Y.; Howard, M.; Schall, T.; Miao, Z. Preparation of Disubstituted Benzamides for Modulating the G Protein-Coupled Receptor (CCXCKR2) Activity and Angiogenesis. WO2005074645, 2005.

(18) Melikian, A.; Wright, J. J. K. Preparation of Benzamide Derivatives as Modulators of Chemokine Receptors for Treatment of Cancer. US20060074071A1, 2006.

(19) Leleti, M. R.; Thomas, W. D.; Zhang, P.; Pennell, A. M. K. Preparation of Chromenopyrazoles, Pyrroloquinolines and their Analogs as Chemokine Receptor CXCR4 and CXCR7 Inhibitors. WO2007115232A2, 2007.

(20) Melikian, A.; Wright, J. J.; Krasinski, A.; Hu, C.; Novack, A. Preparation of Substituted 4-Quinolones and Naphthyridin-4-ones as Chemokine Receptor CCXCKR2 Antagonists. WO2007059108, 2007.

(21) Melikian, A.; Wright, J. J. K.; Krasinski, A. Preparation of N-Pyrrolidinylmethyl- and N-Imidazolylmethyl-N-Phenylmethallylbenzamides as CCXCKR2 Chemokine Receptor Antagonists. WO2007002842, 2007.

(22) Thomas, W. D.; Leleti, M. R.; Pennell, A. M. K. Preparation of Indoles, Indazoles, Benzimidazoles and their Analogs as Chemokine Receptor CXCR4 and CCR7 Inhibitors. WO2007115231A2, 2007.

(23) Clark, M. P.; Lockwood, M. A.; Wagner, F. F.; Natchus, M. G.; Doroh, B. C. Preparation of Substituted Benzohydrazides as Chemokine Receptor Modulators. WO2008112156, 2008.

(24) Chen, X.; Fan, P.; Gleason, M. M.; Jaen, J. C.; Li, L.; McMahon, J. P.; Powers, J.; Zeng, Y.; Zhang, P. Diazepane Derivatives as CXCR7 Modulators and their Preparation, Pharmaceutical Compositions and Use in the Treatment of Diseases. WO2010054006, 2010.

(25) Fretz, H.; Gude, M.; Guerry, P.; Kimmerlin, T.; Lehembre, F.; Pfeifer, T.; Valdenaire, A. 1-[M-Carboxamido(hetero)aryl-methyl]piperidine-4-carboxamide Derivatives as CXCR7 Modulators and their Preparation. US20130345199A1, 2013.

(26) Fretz, H.; Guerry, P.; Kimmerlin, T.; Lehembre, F.; Pothier, J.; Siendt, H.; Valdenaire, A. Preparation of Isoquinolinylalkanamides as CXCR7 Receptor Modulators. WO2014191929, 2014.

(27) Fan, J.; Krasinski, A.; Lange, C. W.; Lui, R. M.; McMahon, J. P.; Powers, J. P.; Zeng, Y.; Zhang, P. Preparation of Pyrrolidinylazolopyrazine Derivatives as CXCR7 Antagonists. WO2014085490A1, 2014.

(28) Gravel, S.; Malouf, C.; Boulais, P. E.; Berchiche, Y. A.; Oishi, S.; Fujii, N.; Leduc, R.; Sinnett, D.; Heveker, N. The peptidomimetic CXCR4 antagonist TC14012 recruits beta-arrestin to CXCR7: roles of receptor domains. *J. Biol. Chem.* **2010,** *285* (49), 37939-37943.

(29) Mungalpara, J.; Thiele, S.; Eriksen, O.; Eksteen, J.; Rosenkilde, M. M.; Vabeno, J. Rational design of conformationally constrained cyclopentapeptide antagonists for C-x-C chemokine receptor 4 (CXCR4). *J. Med. Chem.* **2012,** *55* (22), 10287-10291.

(30) Demmer, O.; Frank, A. O.; Hagn, F.; Schottelius, M.; Marinelli, L.; Cosconati, S.; Brack-Werner, R.; Kremb, S.; Wester, H. J.; Kessler, H. A conformationally frozen peptoid boosts CXCR4 affinity and anti-HIV activity. *Angew. Chem. Int. Ed. Engl.* **2012,** *51* (32), 8110-8113.

(31) Oishi, S.; Fujii, N. Peptide and peptidomimetic ligands for CXC chemokine receptor 4 (CXCR4). *Org. Biomol. Chem.* **2012,** *10* (30), 5720-5731.

(32) Ehrlich, A.; Ray, P.; Luker, K. E.; Lolis, E. J.; Luker, G. D. Allosteric peptide regulators of chemokine receptors CXCR4 and CXCR7. *Biochem. Pharmacol.* **2013,** *86* (9), 1263-1271.

(33) Oishi, S.; Kuroyanagi, T.; Kubo, T.; Montpas, N.; Yoshikawa, Y.; Misu, R.; Kobayashi, Y.; Ohno, H.; Heveker, N.; Furuya, T.; Fujii, N. Development of novel CXC chemokine receptor 7 (CXCR7) ligands: selectivity switch from CXCR4 antagonists with a cyclic pentapeptide scaffold. *J. Med. Chem.* **2015,** *58* (13), 5218-5225.

(34) Craik, D. J.; Fairlie, D. P.; Liras, S.; Price, D. The future of peptide-based drugs. *Chem. Biol. Drug Des.* **2013,** *81* (1), 136-147.

(35) Fosgerau, K.; Hoffmann, T. Peptide therapeutics: current status and future directions. *Drug Discov. Today* **2015,** *20* (1), 122-128.

(36) Behrendt, R.; White, P.; Offer, J. Advances in Fmoc solid-phase peptide synthesis. *J. Pept. Sci.* **2016,** *22* (1), 4-27.

(37) Price, D. A.; Eng, H.; Farley, K. A.; Goetz, G. H.; Huang, Y.; Jiao, Z.; Kalgutkar, A. S.; Kablaoui, N. M.; Khunte, B.; Liras, S.; Limberakis, C.; Mathiowetz, A. M.; Ruggeri, R. B.; Quan, J. M.; Yang, Z. Comparative pharmacokinetic profile of cyclosporine (CsA) with a decapeptide and a linear analogue. *Org. Biomol. Chem.* **2017,** *15* (12), 2501-2506.

(38) Zabel, B. A.; Wang, Y.; Lewen, S.; Berahovich, R. D.; Penfold, M. E.; Zhang, P.; Powers, J.; Summers, B. C.; Miao, Z.; Zhao, B.; Jalili, A.; Janowska-Wieczorek, A.; Jaen, J. C.; Schall, T. J. Elucidation of CXCR7-mediated signaling events and inhibition of CXCR4-mediated tumor cell transendothelial migration by CXCR7 ligands. *J. Immunol.* **2009,** *183* (5), 3204-3211.

(39) Bassoni, D. L.; Raab, W. J.; Achacoso, P. L.; Loh, C. Y.; Wehrman, T. S. Measurements of beta-arrestin recruitment to activated seven transmembrane receptors using enzyme complementation. *Methods Mol. Biol.* **2012,** *897*, 181-203.

(40) Di, L.; Whitney-Pickett, C.; Umland, J. P.; Zhang, H.; Zhang, X.; Gebhard, D. F.; Lai, Y.; Federico, J. J., 3rd; Davidson, R. E.; Smith, R.; Reyner, E. L.; Lee, C.; Feng, B.; Rotter, C.; Varma, M. V.; Kempshall, S.; Fenner, K.; El-Kattan, A. F.; Liston, T. E.; Troutman, M. D. Development of a new permeability assay using low-efflux MDCKII cells. *J. Pharm. Sci.* **2011,** *100* (11), 4974-4985.

(41) Goetz, G. H.; Farrell, W.; Shalaeva, M.; Sciabola, S.; Anderson, D.; Yan, J.; Philippe, L.; Shapiro, M. J. High throughput method for the indirect detection of intramolecular hydrogen bonding. *J. Med. Chem.* **2014,** *57* (7), 2920-2929.

(42) Sciabola, S.; Goetz, G. H.; Bai, G.; Rogers, B. N.; Gray, D. L.; Duplantier, A.; Fonseca, K. R.; Vanase-Frawley, M. A.; Kablaoui, N. M. Systematic N-methylation of oxytocin: impact

on pharmacology and intramolecular hydrogen bonding network. *Bioorg. Med. Chem.* **2016,** *24* (16), 3513-3520.

(43) Goetz, G. H.; Philippe, L.; Shapiro, M. J. EPSA: a novel supercritical fluid chromatography technique enabling the design of permeable cyclic peptides. *ACS Med. Chem. Lett.* **2014,** *5* (10), 1167-1172.

(44) Gombert, F. O.; Lederer, A.; Obrecht, D.; Romagnoli, B.; Bisang, C.; Ludin, C. Template-fixed Peptidomimetics with CXCR7 Modulating Activity. WO2011095220, 2011.

(45) Wu, B.; Chien, E. Y.; Mol, C. D.; Fenalti, G.; Liu, W.; Katritch, V.; Abagyan, R.; Brooun, A.; Wells, P.; Bi, F. C.; Hamel, D. J.; Kuhn, P.; Handel, T. M.; Cherezov, V.; Stevens, R. C. Structures of the CXCR4 chemokine GPCR with small-molecule and cyclic peptide antagonists. *Science* **2010,** *330* (6007), 1066-1071.

(46) Simon, R. J.; Kania, R. S.; Zuckermann, R. N.; Huebner, V. D.; Jewell, D. A.; Banville, S.; Ng, S.; Wang, L.; Rosenberg, S.; Marlowe, C. K.; Spellmeyer, D. C.; Tans, R.; Frankel, A. D.; Santi, D. V.; Cohen, F. E.; Bartlett, P. A. Peptoids: a modular approach to drug discovery. *Proc. Natl. Acad. Sci. U. S. A.* **1992,** *89* (20), 9367-9371.

(47) Olsen, C. A.; Montero, A.; Leman, L. J.; Ghadiri, M. R. Macrocyclic peptoid-peptide hybrids as inhibitors of class I histone deacetylases. *ACS Med. Chem. Lett.* **2012,** *3* (9), 749-753.

(48) Schwochert, J.; Turner, R.; Thang, M.; Berkeley, R. F.; Ponkey, A. R.; Rodriguez, K. M.; Leung, S. S.; Khunte, B.; Goetz, G.; Limberakis, C.; Kalgutkar, A. S.; Eng, H.; Shapiro, M. J.; Mathiowetz, A. M.; Price, D. A.; Liras, S.; Jacobson, M. P.; Lokey, R. S. Peptide to peptoid

substitutions increase cell permeability in cyclic hexapeptides. *Org. Lett.* **2015,** *17* (12), 2928-2931.

(49) Ovadia, O.; Linde, Y.; Haskell-Luevano, C.; Dirain, M. L.; Sheynis, T.; Jelinek, R.; Gilon, C.; Hoffman, A. The effect of backbone cyclization on PK/PD properties of bioactive peptide-peptoid hybrids: the melanocortin agonist paradigm. *Bioorg. Med. Chem.* **2010,** *18* (2), 580-589.

(50) Rand, A. C.; Leung, S. S.; Eng, H.; Rotter, C. J.; Sharma, R.; Kalgutkar, A. S.; Zhang, Y.; Varma, M. V.; Farley, K. A.; Khunte, B.; Limberakis, C.; Price, D. A.; Liras, S.; Mathiowetz, A. M.; Jacobson, M. P.; Lokey, R. S. Optimizing PK properties of cyclic peptides: the effect of side chain substitutions on permeability and clearance. *MedChemComm* **2012,** *3* (10), 1282-1289.

(51) White, T. R.; Renzelman, C. M.; Rand, A. C.; Rezai, T.; McEwen, C. M.; Gelev, V. M.; Turner, R. A.; Linington, R. G.; Leung, S. S.; Kalgutkar, A. S.; Bauman, J. N.; Zhang, Y.; Liras, S.; Price, D. A.; Mathiowetz, A. M.; Jacobson, M. P.; Lokey, R. S. On-resin N-methylation of cyclic peptides for discovery of orally bioavailable scaffolds. *Nat. Chem. Biol.* **2011,** *7* (11), 810-817.

(52) Cui, J. J.; Araldi, G. L.; Reiner, J. E.; Reddy, K. M.; Kemp, S. J.; Ho, J. Z.; Siev, D. V.; Mamedova, L.; Gibson, T. S.; Gaudette, J. A.; Minami, N. K.; Anderson, S. M.; Bradbury, A. E.; Nolan, T. G.; Semple, J. E. Non-covalent thrombin inhibitors featuring P3-heterocycles with P1-bicyclic arginine surrogates. *Bioorg. Med. Chem. Lett.* **2002,** *12* (20), 2925-2930.

(53) Masic, L. P. Arginine mimetic structures in biologically active antagonists and inhibitors. *Curr. Med. Chem.* **2006,** *13* (30), 3627-3648.

(54) Wang, C. K.; Northfield, S. E.; Swedberg, J. E.; Colless, B.; Chaousis, S.; Price, D. A.; Liras, S.; Craik, D. J. Exploring experimental and computational markers of cyclic peptides: charting islands of permeability. *Eur. J. Med. Chem.* **2015,** *97*, 202-213.

(55) Furukawa, A.; Townsend, C. E.; Schwochert, J.; Pye, C. R.; Bednarek, M. A.; Lokey, R. S. Passive membrane permeability in cyclic peptomer scaffolds is robust to extensive variation in side chain functionality and backbone geometry. *J. Med. Chem.* **2016,** *59* (20), 9503-9512.

(56) Hess, S.; Ovadia, O.; Shalev, D. E.; Senderovich, H.; Qadri, B.; Yehezkel, T.; Salitra, Y.; Sheynis, T.; Jelinek, R.; Gilon, C.; Hoffman, A. Effect of structural and conformation modifications, including backbone cyclization, of hydrophilic hexapeptides on their intestinal permeability and enzymatic stability. *J. Med. Chem.* **2007,** *50* (24), 6201-6211.

(57) Chatterjee, J.; Gilon, C.; Hoffman, A.; Kessler, H. N-methylation of peptides: a new perspective in medicinal chemistry. *Acc. Chem. Res.* **2008,** *41* (10), 1331-1342.

(58) Ovadia, O.; Greenberg, S.; Chatterjee, J.; Laufer, B.; Opperer, F.; Kessler, H.; Gilon, C.; Hoffman, A. The effect of multiple N-methylation on intestinal permeability of cyclic hexapeptides. *Mol. Pharm.* **2011,** *8* (2), 479-487.

(59) Chatterjee, J.; Rechenmacher, F.; Kessler, H. N-methylation of peptides and proteins: an important element for modulating biological functions. *Angew. Chem. Int. Ed. Engl.* **2013,** *52* (1), 254-269.

(60) Wang, C. K.; Northfield, S. E.; Colless, B.; Chaousis, S.; Hamernig, I.; Lohman, R. J.; Nielsen, D. S.; Schroeder, C. I.; Liras, S.; Price, D. A.; Fairlie, D. P.; Craik, D. J. Rational design

and synthesis of an orally bioavailable peptide guided by NMR amide temperature coefficients. *Proc. Natl. Acad. Sci. U. S. A.* **2014,** *111* (49), 17504-17509.

(61) Hosea, N. A.; Collard, W. T.; Cole, S.; Maurer, T. S.; Fang, R. X.; Jones, H.; Kakar, S. M.; Nakai, Y.; Smith, B. J.; Webster, R.; Beaumont, K. Prediction of human pharmacokinetics from preclinical information: comparative accuracy of quantitative prediction approaches. *J. Clin. Pharmacol.* **2009,** *49* (5), 513-533.

(62) Cao, X.; Gibbs, S. T.; Fang, L.; Miller, H. A.; Landowski, C. P.; Shin, H. C.; Lennernas, H.; Zhong, Y.; Amidon, G. L.; Yu, L. X.; Sun, D. Why is it challenging to predict intestinal drug absorption and oral bioavailability in human using rat model. *Pharm. Res.* **2006,** *23* (8), 1675-1686.

(63) Riccardi, K.; Cawley, S.; Yates, P. D.; Chang, C.; Funk, C.; Niosi, M.; Lin, J.; Di, L. Plasma protein binding of challenging compounds. *J. Pharm. Sci.* **2015,** *104* (8), 2627-2636.

TOC SYNOPSIS